Journal of Hydroscience and Hydraulic Engineering
Vol. 17, No.2 November, 1999, 107-126

ESTIMATING INSTANTANEOUS TURBULENT BOTTOM SHEAR STRESS UNDER IRREGULAR WAVES

By

Mustafa Ataus SAMAD

M. Eng., Research Associate, Department of Civil Eng. Tohoku University, Aobayama 06, Aoba-ku, Sendai 980-8579, Japan, Email: samad@kasen1.civil.tohoku.ac.jp

and

Hitoshi TANAKA

D. Eng., Professor, Ditto, Email: tanaka@tsunami2.civil.tohoku.ac.jp

SYNOPSIS

A method has been proposed to compute instantaneous turbulent bottom shear stress from the variation in free stream velocity under irregular waves for plane bed condition. Instantaneous free stream velocity and a modified relationship for turbulent wave friction factor have been introduced as the basis for the correlation with bottom shear stress. Turbulent friction factor and phase difference, obtained through spectral analysis of generated free stream velocity time variation and corresponding bottom shear stress from k-ε model results, corresponds quite well to those from laboratory data for sinusoidal waves. Instantaneous bottom shear stress computed by the proposed method has been compared with those from k-ε model results. Proposed method presents a high degree of accuracy and has been found to be very convenient to use from the viewpoint of practical application.

INTRODUCTION

Waves propagating in oceanic regions of shallow and intermediate depths interact with the changing depth. While waves are affected due to shoaling and refraction, the effect of waves on the bottom can be observed through sand movement at the bottom. The sediment movement is caused partly by the process of energy dissipation that takes place through a thin boundary layer attached to the bottom. Flow in this layer is strongly shared through the production and dissipation of turbulent energy, and governs near bottom flow dynamics. This has attracted many researchers to investigate flow properties in the bottom boundary layer. The early experimental studies mainly investigated the mean flow properties in the boundary layer (Jonsson, 1963) and

wave friction factors (Kamphuis, 1975). While detailed turbulent behavior and fine flow visualization techniques are generally applied in recent experiments (Hino et al., 1976; Hayashi and Ohashi, 1982; Sleath, 1987; Jensen et al., 1989) covering both smooth and rough bottom conditions. However, most of these studies considered boundary layer flows induced by sinusoidal oscillation at the free stream.

Apart from the experimental studies, several researchers have proposed mathematical models to estimate boundary layer flows under oscillatory motion. These models mainly use linearized boundary layer equation coupled with turbulence models of various level of complexities; like eddy-viscosity model (Kajiura, 1968), one-equation model (Justesen and Fredsøe, 1985), two-equaiton model (Justesen, 1988a; Asano et al., 1988; Justesen and Spalart, 1990), Reynolds stress model (Sheng, 1982) etc. Also Spalart and Baldwin (1989) had performed direct numerical simulation (DNS) of full Navier-Stokes equation to compute boundary layer flows under sinusoidal wave motion. Among these models, two-equation k-ε model has been the most popular. The k-ε models were originally proposed for unidirectional flows, however its successful use in oscillatory motion is mainly due to the fact that considering turbulent time scales, the flow over most of the domain can be assumed as quasi-steady. Sana and Tanaka (1996) had tested the applicability of different k-ε models and compared model results with DNS data of Spalart and Baldwin (1989) covering a wide range of Reynolds numbers. It was shown that among the models tested, original low Reynolds number model of Jones and Launder (1972) provided the best predictive capability.

Considering the random nature of ocean waves and complexities in determining the governing forcing for sediment transport beneath irregular waves, it is of practical importance that these are studied in full details to facilitate establishing methods for practical computation. Although several researchers have considered non-linearity in wave motion and subsequently studied bottom boundary layer flows (Elfrink et al., 1993; Nadaoka et al., 1994; Tanaka et al., 1998a), only few studies have so far been reported on irregular wave bottom boundary layers. Simons et al. (1994) had measured time variation of bottom shear stress under irregular waves in a two-dimensional wave basin for waves alone and for superimposed currents. This experiment provides some useful information on time variation of bottom shear stress. Madsen et al. (1988) had proposed an analytical model to evaluate irregular wave bottom friction considering spectral wave dissipation based on linearized boundary layer equation, a constant eddy viscosity and directional wave spectrum. Myrhaug (1995) expressed irregular wave friction factor with an assumption that wave motion can be expressed as Gaussian narrow-band random process. All these studies were aimed at expressing irregular wave behavior in the boundary layer in terms of representative spectral properties. Recently Samad and Tanaka (1998) had studied the time varying character of bottom boundary layer using Jones and Launder original low Reynolds number k-ε model and had obtained generally satisfactory results for turbulent computation.

Turbulence modeling can aid resolve detailed time variation of bottom shear stress and turbulent fluctuations, however, it is not always very convenient for practical applicability specially considering computational economy. Alternatively several researchers have tried to achieve simple description of time variation of turbulent bottom shear stress under oscillatory waves that can easily be adopted for practical computation purposes. Hasselmann and Collins (1968), and later Kabling and Sato (1994) had suggested that the time variation of turbulent bottom shear stress can be estimated from the variation of free stream velocity based on the definition of wave friction factor. However, systematic assessment of applicability of such a relationship is yet to be reported. One of the reason for this had been the lack of experimental and computational data on irregular wave bottom shear stress.

In the present paper a detailed spectral analysis has been made to evaluate correlation

characters between free stream velocity and turbulent plane bed bottom shear stress obtained through irregular wave generation and from computed k-ε model results respectively. The analysis has resulted in a systematic evaluation of turbulent wave friction factor, based on which a method to compute instantaneous bottom shear stress has been proposed. When applied with average turbulent phase difference, the proposed method could predict instantaneous turbulent bottom shear stress from free stream velocity with significant accuracy. It has also been observed that the wave friction factor achieved through spectral analysis corresponds quite well to those from experimental data and from computed results for sinusoidal waves.

COMPUTATION METHODOLOGY AND GOVERNING EQUATIONS

In this paper irregular wave free stream velocity time variation has first been generated from input spectral parameters, and the results for spectral density and transfer functions have been compared with those obtained from applying small amplitude wave theory. Upon satisfactory comparison the generated irregular wave velocity record has been specified as free stream velocity to evaluate the pressure term in the boundary layer equation. Original low Reynolds number k-ε model of Jones and Launder (1972) then has been used to compute the bottom shear stress. A detailed spectral analysis has been performed between generated free stream velocity and computed bottom shear stress that resulted in the determination of coherence and phase difference, a description of wave friction factor and a set of correlating coefficient and exponent. The later two has been applied to derive a working relationship between free stream velocity and bottom shear stress. Obtained time variation of bottom shear stress from the proposed method then has been compared with k-ε model results and the accuracy of prediction has been discussed.

Generation of Irregular Wave Free Stream Velocity

The spectral density for irregular water surface elevation, $S_\eta(f)$, can be computed using Bretschneider-Mitsuyasu (Mitsuyasu, 1970) spectral density formulation:

$$S_\eta(f) = 0.257 H_{1/3}^2 T_{1/3} (T_{1/3} f)^{-5} \exp\left\{-1.03 (T_{1/3} f)^{-4}\right\} \tag{1}$$

where, $H_{1/3}$, $T_{1/3}$ = significant wave height and period respectively, and f = frequency of component waves. Applying small amplitude wave theory following relationship can be obtained for spectral densities of water surface elevation and free stream velocity:

$$S_U(f) = H_U^2(f) S_\eta(f) = \left(\frac{\omega}{\sinh 2\pi h/L}\right)^2 S_\eta(f) \tag{2}$$

where, $S_U(f)$ = spectral density of free stream velocity, $H_U(f)$ = velocity transfer function, h = water depth, and L, ω ($=2\pi f$) = wave length and angular frequency of component waves.

Obtained velocity spectrum has then been used to generate velocity time variation with the approximation that irregular waves can be resolved as a sum of infinite number of wavelets with small amplitudes and random phases:

$$U(t) = \sum_i A_{Ui} \cos\left(2\pi f_i t + \phi_i\right) \tag{3}$$

$$A_{Ui} = 2\sqrt{S_U(f)\Delta f_i} \tag{4}$$

where, $U(t)$ = instantaneous free stream velocity, A_{Ui} = velocity amplitudes of component waves, f_i = component frequencies, t = time, ϕ_i = component phases and Δf_i = frequency increment between successive wave components.

k-ε Model

Linearized boundary layer equation has been applied for flow computation in the bottom layer:

$$\frac{\partial u}{\partial t} = -\frac{1}{\rho}\frac{\partial p}{\partial x} + \frac{1}{\rho}\frac{\partial \tau}{\partial z} \tag{5}$$

where, u = velocity in the direction of flow, p = pressure, τ = shear stress, ρ = mass density of the fluid and x-, z- = coordinates along and perpendicular to the direction of flow, respectively. The pressure term in the right hand side can be evaluated from the consideration that outside boundary layer the shear stress vanishes and the velocity approaches free stream velocity. The shear stress for turbulent flow regime can be defined based on kinematic and turbulent eddy viscosity; so that:

$$\frac{\tau}{\rho} = \nu\frac{\partial u}{\partial z} - \overline{u'v'} \tag{6}$$

where, ν = kinematic viscosity and $-\overline{u'v'}$ = Reynolds stress which is:

$$-\overline{u'v'} = \nu_t \frac{\partial u}{\partial z} \tag{7}$$

where, ν_t = turbulent eddy viscosity which again can be expressed in terms of the turbulent kinetic energy, k and its dissipation rate ε:

$$\nu_t = C_\mu f_\mu \frac{k^2}{\varepsilon} \tag{8}$$

where C_μ, f_μ = parameters determined from experimental results.

The closure is achieved by introducing transport equations for k and ε. These are given by:

$$\frac{\partial k}{\partial t} = \frac{\partial}{\partial z}\left\{\left(\nu + \frac{\nu_t}{\sigma_k}\right)\frac{\partial k}{\partial z}\right\} + \nu_t\left(\frac{\partial u}{\partial z}\right)^2 - \varepsilon - D \tag{9}$$

$$\frac{\partial \varepsilon}{\partial t} = \frac{\partial}{\partial z}\left\{\left(\nu + \frac{\nu_t}{\sigma_\varepsilon}\right)\frac{\partial \varepsilon}{\partial z}\right\} + C_1 f_1 \nu_t \frac{\varepsilon}{k}\left(\frac{\partial u}{\partial z}\right)^2 - C_2 f_2 \frac{\varepsilon^2}{k} + E \tag{10}$$

where, σ_k, D, σ_ε, C_1, f_1, C_2, f_2, E = model parameters. Equations (5) through (10) are solved numerically to obtain time variation of turbulent flow quantities and the bottom shear stress.

In the present computation, original low Reynolds number k-ε model of Jones and Launder (1972) has been used. The selection of this particular model has been based on the testing of low

Reynolds number k-ε models by Sana and Tanaka (1996). For numerical computation, the governing equations have been made non-dimensional form and Crank-Nicolson implicit finite difference scheme has been applied. In the non-dimensional form of the governing equations, along with free stream velocity variation only Reynolds number and reciprocal of Strouhal number (S) are required to compute flows in laminar, turbulent or in transitional regimes (where, $S=U_{1/3}/z_h\omega_{1/3}$, $U_{1/3}$ = significant free stream velocity, $\omega_{1/3}$ = wave frequency corresponding to significant wave period and z_h = a normalizing depth set outside boundary layer).

Non-Dimensional Parameter

Irregular wave Reynolds number ($\mathrm{Re}_{1/3}$) has been defined in terms of significant wave properties and has been made analogous to wave Reynolds number defined by Jonsson (1966):

$$\mathrm{Re}_{1/3} = \frac{U_{1/3}^{\,2}}{\nu\omega_{1/3}} \tag{11}$$

with

$$U_{1/3} = \frac{\pi H_{1/3}}{T_{1/3}} \frac{1}{\sinh\, 2\pi h / L}\,; \qquad \omega_{1/3} = \frac{2\pi}{T_{1/3}} \tag{12}$$

COMPUTATION RESULT AND SPECTRUM ANALYSIS

Input Parameters

The input wave parameters specified for computation have been the significant wave height and period, water depth, and a normalizing depth where the flow is same with the free stream velocity. Input parameters have been selected to produce flows with sufficiently large irregular wave Reynolds number representing turbulent flow. Four turbulent cases have been considered here and the parameters are presented in Table 1. Apart from these cases, additional model runs have also been carried out for sinusoidal waves to examine the applicability of proposed wave friction factor description.

Table 1. Parameters for turbulent irregular wave computation.

Run	h cm	z_h cm	$T_{1/3}$ s	$H_{1/3}$ cm	$U_{1/3}$ cm/s	$\mathrm{Re}_{1/3}$
Case 1	1000	100	10	430	184.0	5.39×10^6
Case 2				480	205.3	6.71×10^6
Case 3				505	216.1	7.43×10^6
Case 4				530	226.7	8.18×10^6

Generation of Free Stream Velocity

Simulation of irregular wave has been performed to generate sufficiently long velocity time series with number of waves being over 150 to facilitate computation of spectral properties. A total of 250 component waves have been considered for which randomly generated frequencies and phases have been used. The accuracy of generated velocity has been checked against input spectrum. Fig.1 shows the comparison of input (Eq.2) spectrum with that from generated data for

Case 1. The wave energy spread has been found to concentrate within a frequency range of 0.05Hz to 0.40Hz or equivalently within the period of 2.5s to 20.0s. Generated velocity spectrum can generally be seen in very good agreement with the input one. For lower frequencies the generated spectrum is slightly over-estimated, however, considering the frequency range with high spectral wave energy, the generated wave series can be considered satisfactory.

Spectral properties of Turbulent Bottom Shear Stress and Free Stream Velocity

Under turbulent motion, the phase difference between the bottom shear stress and the free stream velocity reduces substantially. Accordingly several researchers have suggested the possibility of establishing functional relationship to evaluate bottom shear stress from free stream velocity. Fig.2 shows the correlation between free stream velocity and k-ε model computed bottom shear

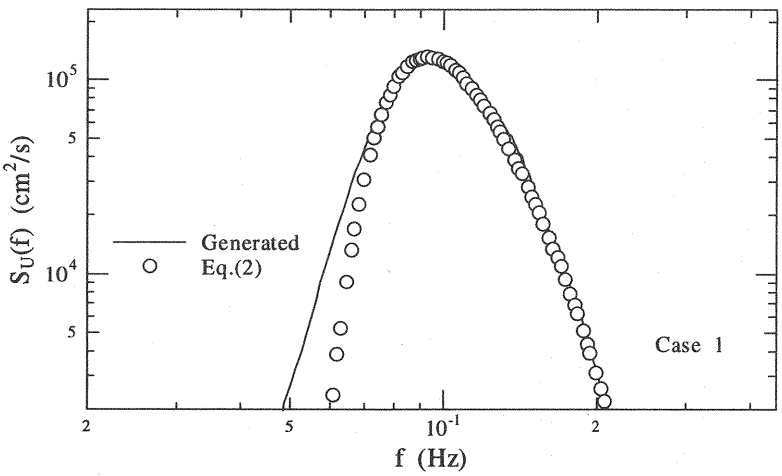

Fig. 1 Comparison of input and generated velcoity spectrum, Case 1

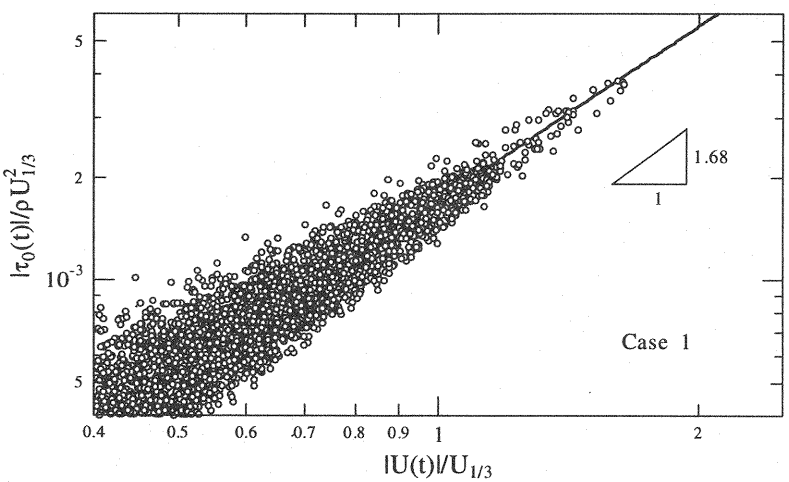

Fig. 2 Variation of bottom shear stress with free stream velocity, Case 1

stress for Case 1. Although the correlating function can be satisfactorily estimated from such a figure, data spread at lower velocities still indicates the importance of turbulent phase difference between the velocity and the bottom shear stress.

One of the popular ways to evaluate wave energy dissipation at the bottom, is through introducing wave friction factor. For irregular waves Hasselmann and Collins (1968) considered energy dissipation by component waves contained in wave spectrum and applied quadratic friction law of Jonsson (1966). It was later argued that while dealing with spectral components Hasselmann and Collins (1968) could overcome the problem of representative waves, however, it was not defined how the spectral wave friction factor is related to bottom roughness. Madsen et al. (1988) proposed an equivalent monochromatic wave to describe the bottom shear stress spectrum which was used along with linearized boundary layer equations and a linear eddy viscosity description to calculate spectral wave attenuation.

In the present analysis a more generalized representation of correlation between bottom shear stress and free stream velocity has been made. This is aimed at providing a description for temporal variation of bottom shear stress. To define the correlation, the authors propose following relation for instantaneous bottom shear stress such that:

$$\frac{\tau_0(t)}{\rho} \propto U(t)|U(t)|^{n-1} \tag{13}$$

where, $\tau_0(t)$ = instantaneous bottom shear stress, $U(t)$ = instantaneous free stream velocity and n = a correlating exponent. In Eq.(13) the constant of proportionality and the exponent can be replaced introducing an extended expression for the wave friction factor.

This functional relationship has been studies through spectrum analysis of generated irregular wave velocity and corresponding k-ε model computed bottom shear stress. Cross-spectrum and coherence have been computed to determine the exponent, 'n', for maximum correlation and, the importance of phase difference is further evaluated. As mentioned before, introduction of wave friction factor can aid determination of the proportionality coefficient in the functional relation, Eq.(13). However, selection of an appropriate wave friction factor for turbulent motion itself becomes an important task to achieve a practically acceptable accuracy. To facilitate this, a transfer function has been defined between the bottom shear stress and the free stream velocity from the spectral analysis, and has been compared with that from k-ε model result.

The spectral density, coherence and phase difference have been computed for different values of 'n'. Fig.3, as an example, shows $S_U{}^{1.68}(f)$, the spectral density for $U(t)|U(t)|^{0.68}$ (or for 'n'=1.68), for Case 1. Corresponding variation in coherence and phase difference between bottom shear stress and free stream velocity are presented in Fig.4 for different exponent values. Computed spectral densities and subsequently the coherence and phase difference result in a range of component frequencies with magnitudes from very small to very high. These extreme frequencies sometime represent practically unrealistic values. In order to subjectively evaluate spectral parameters within a practically meaningful range, frequencies corresponding to 99% of velocity spectrum have been selected for the present analysis. This was also necessary to define average quantities of the same spectral parameters over a suitable range of frequencies to facilitate inter-comparison between different computational cases. The frequency range for 99% of velocity spectrum is also shown in Fig.3. Considering the range of spectral energy spread, the assumption of this limiting frequency seems quite reasonable from the figure.

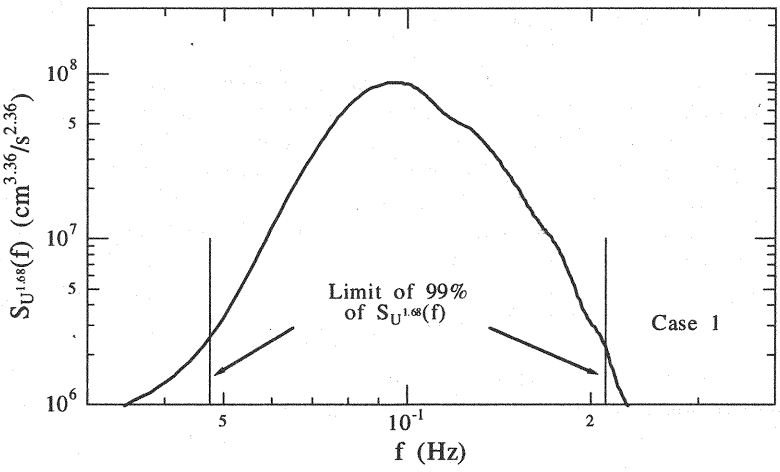

Fig. 3 Spectral density of $U(t)|U(t)|^{0.68}$, for Case 1

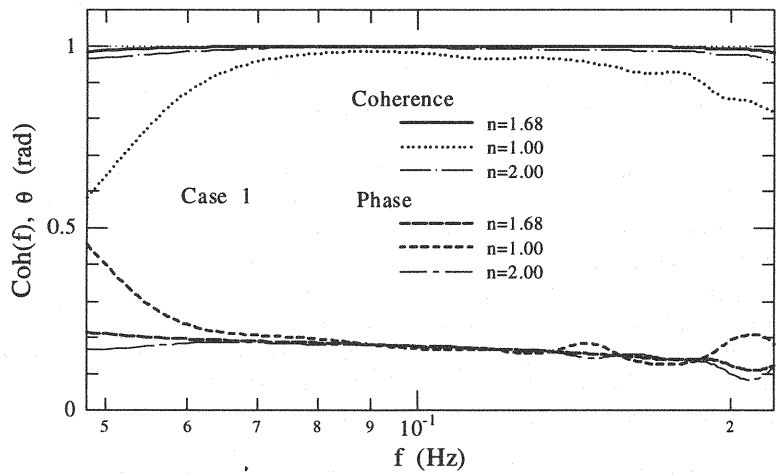

Fig. 4 Coherence and phase difference for different 'n', Case 1

In Fig.4 it can be seen that within the selected frequency range the coherence is almost unity for some exponent values. Whereas the phase difference shows a gradual decrease with increasing frequency. These have been further elaborated by presenting average coherence and phase difference for all cases and for different 'n' values as shown in Figs.5 and 6 respectively. Fig.5 shows that the maximum average coherence can be achieved when n=1.68, implying a maximum correlation between $\tau_0(t)$ and $U(t)$ with an exponent of 1.68. The average phase difference (θ) shows only a small variation with 'n' (Fig.6) and, therefore, has been evaluated as an average from all the cases at n=1.68 resulting in θ=0.16 rad (≈9.2 deg.).

PREDICTION OF BOTTOM SHEAR STRESS

Replacing the proportionality function with a wave friction factor representing temporal

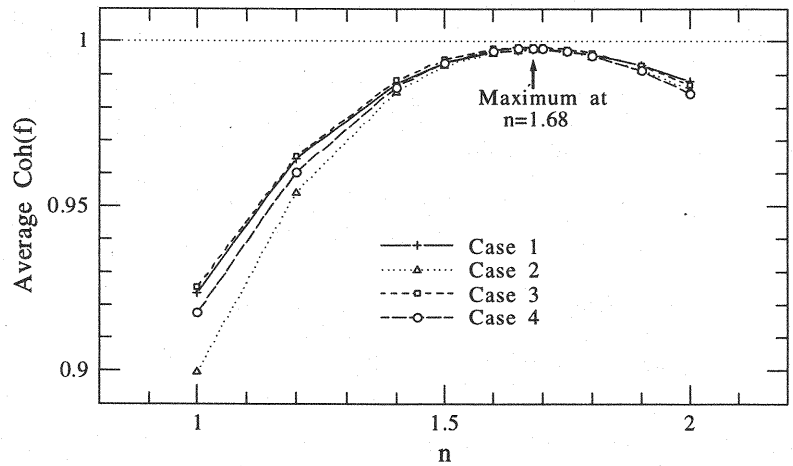

Fig. 5 Average coherence as a function of 'n' for all cases

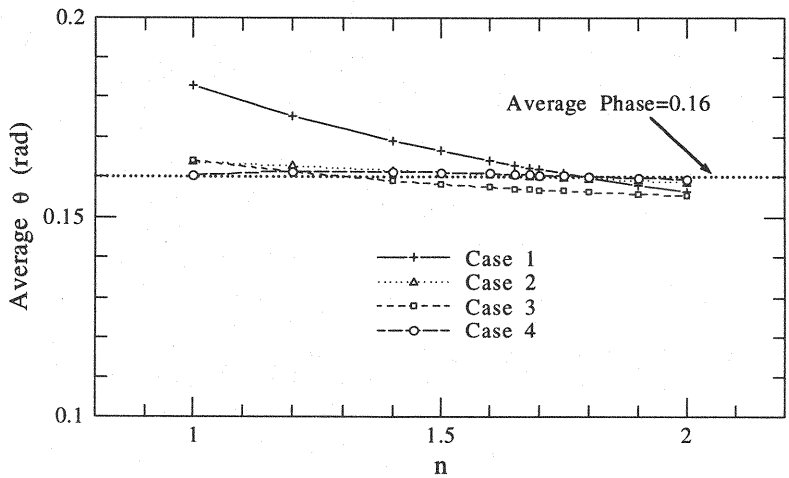

Fig. 6 Variation of averge phase difference as a funciton of 'n'

variation, $f_w(t)$, in Eq.(13), the instantaneous bottom shear stress can be evaluated as:

$$\tau_0(t) = \frac{\rho}{2} f_w(t) U(t) |U(t)| \tag{14}$$

It should be noted that the instantaneous friction factor introduced in Eq.(14) represents temporal variation. As such it is slightly different from the conventional wave friction factor (f_w) proposed by Jonsson (1966) based on the maximum free stream velocity and bottom shear stress.

Wave friction factor itself has been studied extensively by many researchers for sinusoidal wave induced flows (Jonsson, 1966; Kajiura, 1968; Tanaka and Thu, 1984). Fredsøe and Deigaard (1992) have computed f_w for sinusoidal waves integrating the flow momentum over the depth and

have proposed that:

$$f_w = 0.035\,\mathrm{Re}^{-0.16} \tag{15}$$

where Re = wave Reynolds number defined by Jonsson (1966). To facilitate computation for instantaneous quantities, an alternative wave Reynolds number (*RE*) can be introduced corresponding to instantaneous free stream velocity so that:

$$RE = \frac{U(t)^2}{\omega\nu} \tag{16}$$

and subsequently $f_w(t)$ can be defined as:

$$f_w(t) = 0.035\,RE^{-0.16} \tag{17}$$

Now, substituting Eq.(16) in Eq.(17) and replacing $f_w(t)$ in Eq.(14), it is possible to obtain a description for instantaneous bottom shear stress:

$$\tau_0(t) = \frac{\rho}{2} 0.035(\omega\nu)^{0.16} U(t)|U(t)|^{0.68} \tag{18}$$

It is interesting to note that the exponent obtained through spectral analysis matches exactly with that from Eq.(18) when the instantaneous turbulent friction factor is assessed from that analogous to the formulation of Fredsøe and Deigaard (1992).

The proportionality constant, which is $\rho/2$ 0.035 $(\omega\nu)^{0.16}$, alternatively can be evaluated by defining a transfer function between the free stream velocity and the bottom shear stress so that:

$$H_\tau(f) = \frac{\rho}{2} A\,(\omega\nu)^{0.16} \tag{19}$$

where A = a coefficient. The definition is analogous to defining the temporal wave friction factor as, $f_w(t) = A\ RE^{-0.16}$. The coefficient A then can be obtained from the comparison with corresponding transfer function from k-ε model result. The later could be defined as:

$$H_\tau(f) = \sqrt{\frac{S_\tau(f)}{S_{U^{1.68}}(f)}} \tag{20}$$

where $S_\tau(f)$ = spectral density of bottom shear stress. The wave frequency in Eq.(19), $\omega=2\pi f$, has been considered both from component waves and from the frequency corresponding to significant wave period (denoted as Method 2 and Method 3 respectively). From Eq.(19) and Eq.(20), and considering both methods, the coefficient has been achieved as A=0.041. The comparison of transfer functions from these methods along with that from k-ε model is presented in Fig.7. Within the frequency range defined earlier, both methods show reasonably good agreement with k-ε model result.

Obtained magnitude of the coefficient then can be introduced to achieve a revised wave friction factor description:

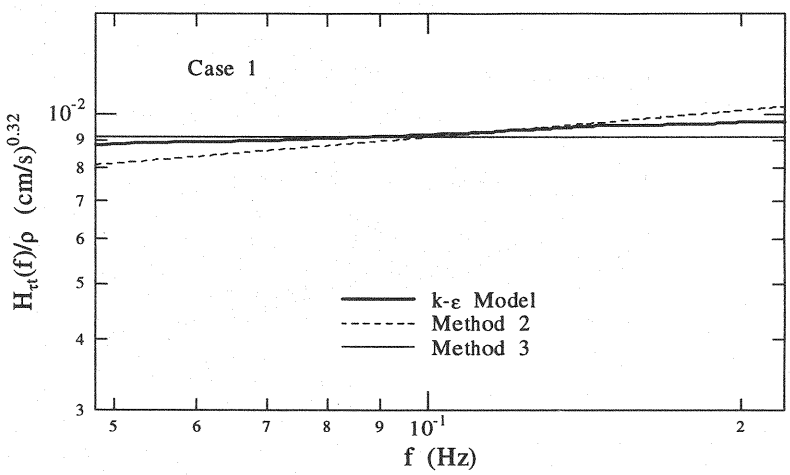

Fig. 7 Comparison of bottom shear stress transfer funciton with k-e model result, Method 2 and Method 3, Case 1

$$f_w(t) = 0.041 RE^{-0.16} \tag{21.a}$$

and analogously,

$$f_w = 0.041 \mathrm{Re}^{-0.16} \tag{21.b}$$

The suitability of this revised friction factor formulation (Eq.21.b) and phase difference (Fig.6) have been compared with available experimental and computation data for sinusoidal waves (Sana, 1997; Jensen et al., 1989; Sawamoto and Sato, 1991), and with smooth turbulent friction factor expressions by Jonsson (1966), Kajiura (1968), Fredsøe and Deigaard (1992), and Tanaka and Thu (1994). These are presented in Figs.8 and 9. To cover the range of Reynolds numbers presented in this paper for irregular waves, additional computations have been performed for sinusoidal wave friction factors and phase differences. Fig.8 shows that the friction factor description obtained by spectral analysis is in very good agreement with experimental and computational data. It also shows better prediction of turbulent friction factor than other methods presented in the figure. Similarly the average phase difference (θ) obtained through spectral analysis also corresponds well with those from sinusoidal waves (Fig.9) for the range of Reynolds number considered.

Determined proportionality function and the exponent now can be inserted in the functional relation (Eq.13) along with the inclusion of turbulent phase difference to achieve an improved description to compute irregular wave instantaneous bottom shear stress.

$$\tau_0(t - \frac{\theta}{\omega}) = \frac{\rho}{2} 0.041 (\omega\nu)^{0.16} U(t)|U(t)|^{0.68} \tag{22}$$

Application of Eq.(22) also requires an appropriate selection of wave frequency. As mentioned earlier, it can either be determined from individual waves in the wave train or from that corresponding to significant wave period. Apart from these, it is also possible to directly apply proposed sinusoidal wave friction factor in Eq.(14) for individual waves to calculate the bottom

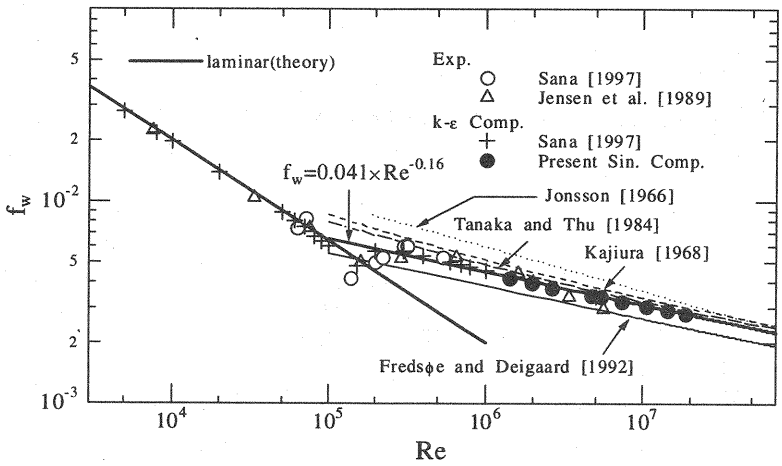

Fig. 8 Comparison of proposed friction factor with existing data and with other methods

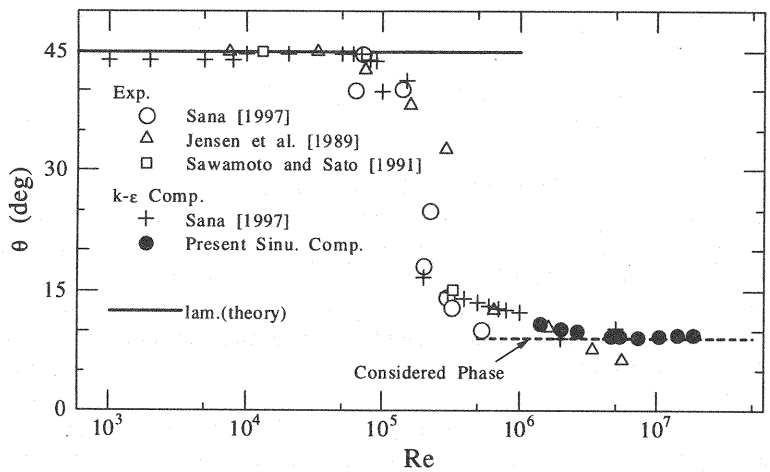

Fig. 9 Comparison of phase difference obtained from spectral abalysis with existing data

shear stress. As such, based on the selection of friction factor and wave frequency, three possible methods to compute instantaneous bottom shear stress could be identified. These methods along with the relationships to compute instantaneous bottom shear stress are presented in Table 2.

Time variation of bottom shear stress obtained by applying these methods have been compared with those from k-ε model results. In an effort to investigate the relative importance and general applicability of the methods, a detailed accuracy analysis also has been performed. It can be mentioned here that out of these three possible methods, Method 3 presents the most easy to use formulation from practical application standpoint.

Accuracy of Prediction

Bottom shear stress calculated through proposed methods have been compared with k-ε model results. As mentioned earlier, k-ε models have mainly been proposed for unidirectional flows and its use in oscillatory flow is relatively recent. However, its application to oscillatory flows by different researchers showed very satisfactory results in bottom shear stress computation. For sinusoidal wave computations Asano et al. (1988), Justesen (1988b), Justesen and Spalart (1990), Sana and Tanaka (1996) very successfully applied k-ε models and achieved very good results. A comprehensive review of turbulence models applied to sinusoidal waves was published by Sleath (1990). It was noted that k-ε models generally provide very good prediction of turbulent bottom shear stress.

For non-linear waves Tanaka et al. (1998b) have applied low Reynolds number k-ε model of Jones and Launder (1972) for flow computations in the boundary layer and showed satisfactory prediction of flow properties. Sana and Tanaka (1996) also considered one case of flat crested non-sinusoidal flow scenario for which DNS data from Spalart and Baldwin (1989) was available. The prediction of bottom shear stress was remarkably well through k-ε model computation.

In view of these studies, the authors felt it appropriate to lay sufficient confidence on low Reynolds number k-ε models in their ability to predict bottom shear stress within the range of accuracy warranted for practical application. Such that, the accuracy of proposed methods have been compared with k-ε model results.

Comparison between obtained bottom shear stress time series and that from k-ε model results for all the methods are shown in Figs. 10 and 11 for Case 1 and Case 4 respectively. The figures suggest that the accuracy of prediction for Methods 2 and 3 are generally very good, whereas, for Method 1 the deviation from model result is the maximum. In Method 1 the wave friction factor (f_w) for individual waves has been considered corresponding to the average of crest and trough velocities. This might have contributed to the differences observed for Method 1. Also, consideration of sinusoidal wave approximation for individual waves might cause discontinuity in bottom shear stress between successive waves with very high and low velocity amplitudes as can be seen in Fig. 11. During flow reversal the bottom shear stress is slightly underestimated consistently by the proposed methods than those from k-ε model result. However, considering the prediction of peak bottom shear stresses, both Method 2 and Method 3 show very good results indicating that the selection of wave frequency only has a small influence on the prediction.

Table 2. Summary of proposed methods to compute instantaneous turbulent bottom shear stress.

Method	Set of relationships used	Remarks
Method 1	$\tau_0(t-\frac{\theta}{\omega})=\frac{\rho}{2}f_w U(t)\lvert U(t)\rvert$ $f_w = 0.041\,\mathrm{Re}^{-0.16}$ $\mathrm{Re} = U_0^{\,2}/\omega\nu$	F_w : average between crest and trough values for individual waves ω : for individual waves U_0 : from individual waves
Method 2	$\tau_0(t-\frac{\theta}{\omega})=\frac{\rho}{2}0.041(\omega\nu)^{0.16}U(t)\lvert U(t)\rvert^{0.68}$	ω : for individual waves
Method 3	$\tau_0(t-\frac{\theta}{\omega_{1/3}})=\frac{\rho}{2}0.041(\omega_{1/3}\nu)^{0.16}U(t)\lvert U(t)\rvert^{0.68}$	$\omega_{1/3}$: from significant wave period

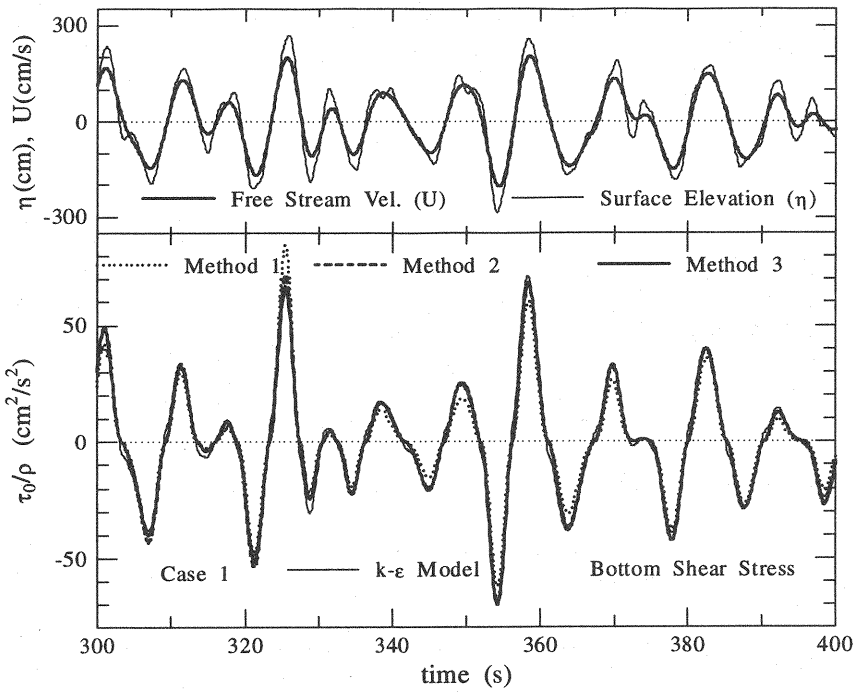

Fig. 10 Comparison of time variation of predicted and k-ε modeled bottom shear stress, Case 1

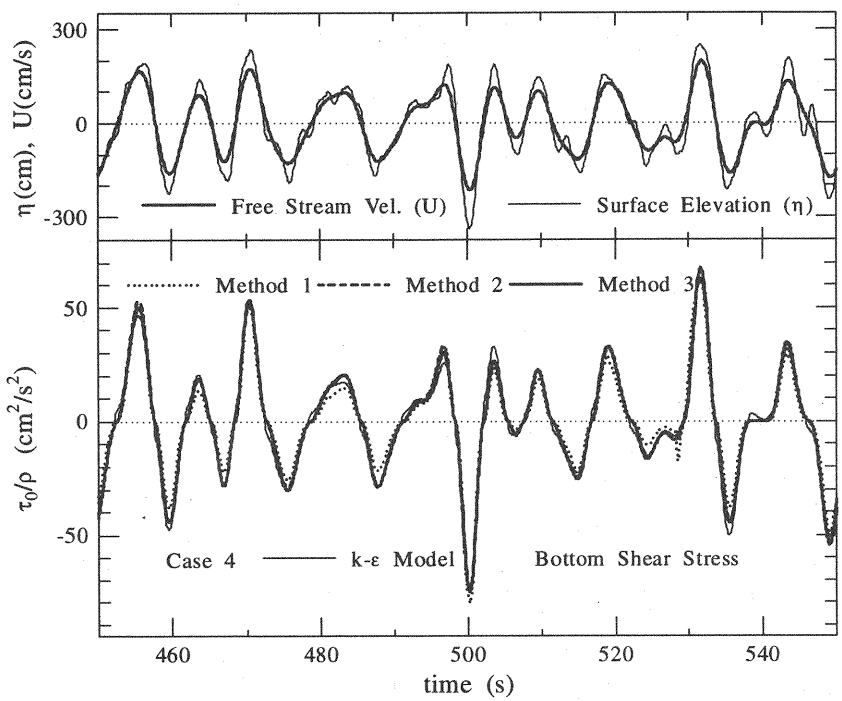

Fig. 11 Comparison of time variation of predicted and k-ε modeled bottom shear stress, Case 4

Figures 12(a), (b) and (c) show the comparison of predicted and computed bottom shear stresses for Method 1, Method 2 and Method 3 respectively. It again can be seen that the level of accuracy for both Method 2 and Method 3 are very high. As observed before, Method 1 shows the largest deviation from the computed results.

A quantitative accuracy of proposed methods has also been performed through the following accuracy factor.

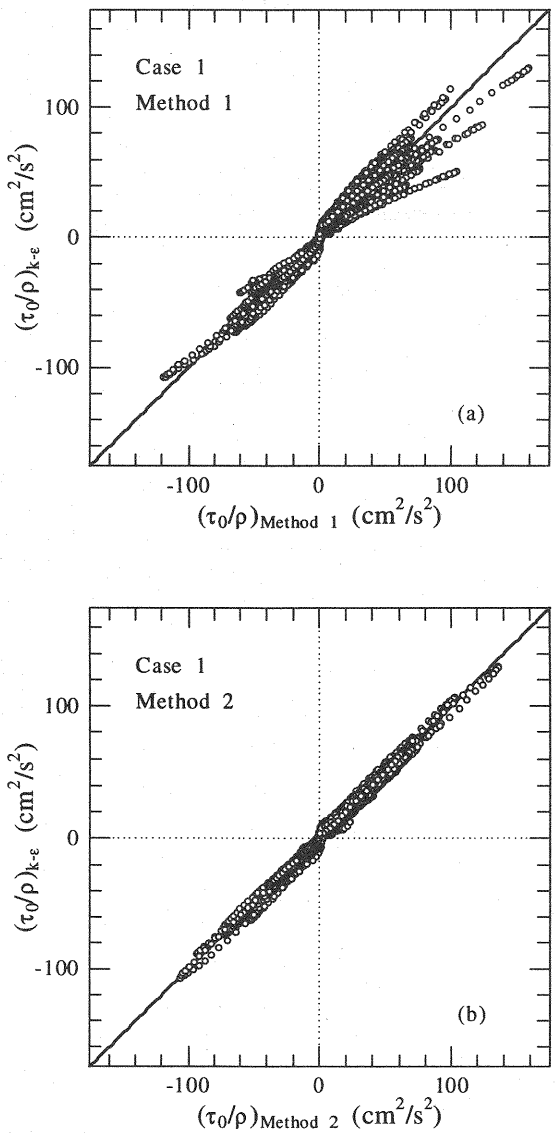

Fig. 12 Accuracy check for predicted bottom shear stress, Case 1;
a) Method 1, b) Method 2 and c) Method 3

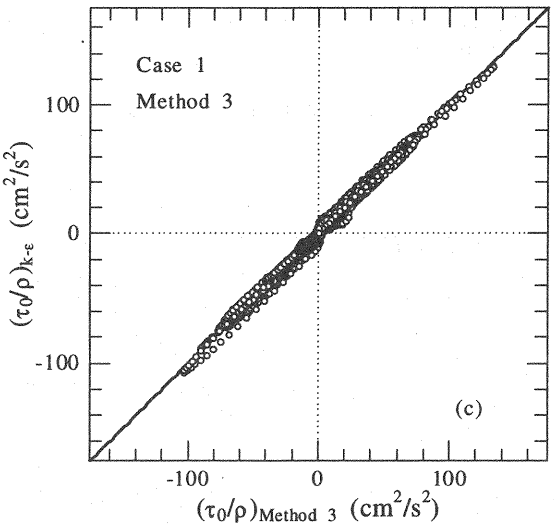

Fig. 12 (Continued) Accuracy check for predicted bottom shear stress, Case 1; a) Method 1, b) Method 2 and c) Method 3

$$F_a = \frac{\tau_{0comp}}{\tau_{0k-\varepsilon}} \tag{23}$$

The standard deviation has been defined as:

$$\sigma = \sqrt{\frac{1}{N-1}\sum_{i=1}^{N}\left(F_{ai} - F_m\right)^2} \tag{24}$$

with

$$F_m = \frac{1}{N}\sum_{i=1}^{N} F_{ai} \tag{25}$$

where τ_{0comp}, $\tau_{0k\text{-}\varepsilon}$ = proposed and k-ε model computed bottom shear stresses respectively, F_m = mean accuracy factor, N = total number of data pairs and i = index subscript. The percentage of the data falling in the range of ±10% and ±20% of the accuracy factor then has been computed. For a perfect agreement with k-ε model result these percentages are 100%.

The accuracy factor has been computed for both instantaneous, $\tau_0(t)$, as well as maximum bottom shear stress, τ_c, in a wave cycle. During flow reversal, bottom shear stress becomes very small and use of Eq.(23) could result in unrealistically small or large values for F_a due to division of two very small numbers in determining F_a (τ_{0comp}, $\tau_{0k\text{-}\varepsilon}$ in this case). Therefore, instantaneous bottom shear stresses with values less than 10% of the significant bottom shear stress have not been considered for accuracy factor computation. For all the cases a total of about 15000 data pairs have been considered with a time step of 0.1s covering about 150 wave cycles. Out of which about 10000 data pairs have been selected for computation of the accuracy factor. Table 3 shows a

summary of accuracy analysis. It shows that both Method 2 and Method 3 have high predictive ability with about 65% $\tau_0(t)$ values lying in ±10% of the accuracy range. For τ_c it is over 80%. It can be seen that Method 3 is not only easy to use for practical purposes but also the most accurate.

It is worth mentioning here that the correlation character and the turbulent phase difference between free stream velocity and bottom shear stress description have been achieved for very high irregular wave Reynolds numbers simulating fully turbulent flow conditions. Accordingly proposed wave friction factor is also applicable for corresponding high Reynolds number ranges. Calculation of instantaneous bottom shear stress using proposed formulation is therefore valid for fully turbulent flow conditions alone.

Table 3. Accuracy of predicted bottom shear stress: % of data in the accuracy range of ±10% and ±20%, and Standard Deviation (σ).

Model Runs	Method 1						Method 2						Method 3					
	Instantaneous			Maximum			Instantaneous			Maximum			Instantaneous			Maximum		
	Accuracy Range (%)			Accuracy Range (%)			Accuracy Range (%)			Accuracy Range (%)			Accuracy Range (%)			Accuracy Range (%)		
	±10 %	±20 %	σ	±10 %	±20 %	σ	±10 %	±20 %	σ	±10 %	±20 %	σ	±10 %	±20 %	σ	±10 %	±20 %	σ
Case 1	23.0	51.5	0.19	40.1	71.2	0.23	64.3	88.2	0.14	76.5	95.5	0.10	66.1	89.2	0.14	82.6	95.5	0.10
Case 2	25.1	52.7	0.22	40.1	66.9	.022	64.9	88.2	0.14	82.2	96.8	0.09	66.8	89.8	0.13	86.7	98.1	0.09
Case 3	21.2	51.5	0.22	29.9	69.5	0.26	62.7	89.1	0.15	76.8	97.4	0.08	67.2	89.9	0.14	86.1	98.0	0.07
Case 4	20.8	50.5	0.24	32.3	67.7	0.24	63.3	88.4	0.14	81.1	96.8	0.09	66.4	89.6	0.14	86.2	96.9	0.09

CONCLUSIONS

A detailed spectral analysis has been performed on irregular wave k-ε model results for turbulent bottom shear stress and free stream velocity for plane bed condition. Their correlation behavior has been analyzed to obtain a working relationship to compute irregular wave instantaneous bottom shear stress from the free stream velocity variation. Obtained correlating exponent and coefficient values also provide description for irregular wave friction factor which corresponds very well with those obtained from sinusoidal waves. The average turbulent phase difference between free stream velocity and bottom shear stress also falls in the same range of corresponding sinusoidal waves.

Following the definition of wave friction factor along with obtained friction factor description three possible methods to compute instantaneous turbulent bottom shear stress have been identified. Prediction by all the methods generally shows very good agreement with k-ε model results. It has been observed that the selection of wave frequency in computing the bottom shear stress has only a small influence on the accuracy of prediction. However, use of significant wave period (Method 3) shows slightly better predictive ability. It is also the most convenient to use in practical applications.

REFERENCES

1) Asano, T., H. Godo and Y. Iwagaki : Oscillatory bottom boundary layer by low Reynolds number turbulence model, Proc. 21st Int. Conf. Coastal Eng., pp.743-755, 1988.
2) Elfrink, B., I.B. Hedegaard, R. Deigaard and J. Fredsøe : Net sediment transport in non-

breaking waves, Prog. Rep.74, Inst. Hydrodynamic and Hyd. Eng., Tech. Univ. Denmark, pp.1-11, 1993.
3) Fredsøe, J. and R. Deigaard : Mechanics of Coastal Sediment Transport, World Scientific, 369p., 1992.
4) Hasselmann, K. and J.I. Collins : Spectral dissipation of finite-depth gravity waves due to turbulent bottom friction, J. Marine Res., Vol.26, pp.1-12, 1968.
5) Hayashi, T. and M. Ohashi : A dynamical and visual study on the oscillatory turbulent boundary layer, In: Turbulent Shear Flows 3, Springer Verlag, pp.18-33, 1982.
6) Hino, M., M. Sawamoto and S. Takasu : Experiments on transition to turbulence in an oscillatory pipe flow, J. Fluid Mech., Vol.75, pp.193-207, 1976.
7) Jensen, B.L., B.M. Sumer and J. Fredsøe : Turbulent oscillatory boundary layer at high Reynolds numbers, J. Fluid Mech., Vol.206, pp.265-297, 1989.
8) Jones, W.P. and B.E. Launder : The prediction of laminarization with a two equation model of turbulence, Int. J. Heat and Mass Transfer, Vol.15, pp.301-314, 1972.
9) Jonsson, I.G. : Measurements in the turbulent wave boundary layer, Proc. 10th Congress of IAHR, Vol.1, pp.85-92, 1963.
10) Jonsson, I.G. : Wave boundary layers and wave friction factors, Proc. 10th Int. Conf. Coastal Eng., pp.27-148, 1966.
11) Jestesen, P. and J. Fredsøe : Distribution of turbulence and suspended sediment in the wave boundary layer, Prog. Rep.62, Inst. Hydrodynamic and Hyd. Eng., Tech. Univ. Denmark, pp.61-67,1985.
12) Justesen, P. and P.R. Spalart : Two equation turbulence modeling of oscillatory boundary layers, Proc. 28th Aerospace Sc. Meeting, AIAA, pp.1-9, 1990.
13) Justesen, P. : Prediction of turbulent oscillatory flow over rough beds, Coastal Eng., Vol.12, pp.257-284, 1988a.
14) Justesen, P. : A model for the smooth wall oscillatory boundary layer flows, Prog. Rep.67, Inst. Hydrodynamic and Hyd. Eng., Tech. Univ. Denmark, pp.23-31, 1988b.
15) Kabling, M.B. and S. Sato : A numerical model for nonlinear waves and beach evolution including swash zone, Coastal Eng. in Japan, JSCE, Vol.37, No.1, pp.67-86, 1994.
16) Kajiura, K. : A model for the bottom boundary layer in water waves, Bull. Earthquake Res. Inst., Vol.45, pp.75-123, 1968.
17) Kamphuis, J.W. : Friction factor under oscillatory waves, J. Waterways, Harbor and Coastal Eng. Division, ASCE, Vol.101, No.WW2, pp.193-203, 1975.
18) Madsen, O.S., Y.K. Poon and H.C. Graber : Spectral wave attenuation by bottom friction: Theory, Proc. 21st Int. Conf. Coastal Eng., pp.492-504, 1988.
19) Mitsuyasu, H. : On the growth of spectrum of wind-generated waves, Proc. 17th Conf. Coastal Eng., JSCE, Vol.17, pp.1-7, 1970. (In Japanese).
20) Myrhaug, D. : Bottom friction beneath random waves, Coastal Eng., Vol.24, pp.259-273, 1995.
21) Nadaoka, K., H. Yagi, Y. Nihei and K. Nomoto : Characteristics of turbulent structure in asymmetric oscillatory flow, Proc. 41st Conf. Coastal Eng., JSCE, Vol.41, pp.141-145, 1994. (In Japanese).
22) Samad, M.A. and H. Tanaka : Oscillatory bottom boundary layer under irregular waves, J. App. Mech., JSCE, Vol.1, pp.747-755, 1998.
23) Sana, A. and H. Tanaka : The testing of low Reynolds number k-ε models by DNS data for an oscillatory boundary layer, Flow Modeling and Turbulence Measurement VI, pp.363-370, 1996.
24) Sana, A. : Experimental and numerical study on turbulent oscillatory boundary layer, D. Eng. Diss., Tohoku Univ., 176p., 1997.
25) Sawamoto, M. and E. Sato : The structure of oscillatory turbulent boundary layer over rough bed, Coastal Eng. in Japan, JSCE, Vol.34, No.1, pp.1-14, 1991.

26) Sheng, Y.P. : Hydraulic applications of a second-order closure model of turbulent transport, Proc. Conf. on Applying Research to Practice, pp.106-119, 1982.
27) Simons, R.R., T.J Grass, W.M. Saleh and M.M. Tehrani : Bottom shear stress under random waves with a current superimposed, Proc. 24th Int. Conf. Coastal Eng., pp.565-578, 1994.
28) Sleath, J.F.A. : Turbulent oscillatory flow over rough beds, J. Fluid Mech., Vol.182, pp.369-409, 1987.
29) Sleath, J.F.A. : Seabed boundary layers, In The Sea (Eds. Le Mehaute, B. and B.M. Hanes), Vol.9 (Part B), pp.693-727, 1990.
30) Spalart, P.R. and B.S. Baldwin : Direct simulation of a turbulent oscillatory boundary layer, In: Turbulent Shear Flows 6, Springer Verlag, pp.417-440, 1989.
31) Tanaka, H., B.M. Sumer and C. Lodahl : Theoretical and experimental investigation on laminar boundary layer under cnoidal wave motion, Coastal Eng. J., Vol.40, No.1, pp.81-98, 1998a.
32) Tanaka, H., A. Sana, H. Yamaji and M.A. Samad : Experimental and numerical investigation on asymmetric oscillatory boundary layers, J. Hydroscience and Hyd. Eng., JSCE, Vol.16, No.1, pp.117-126, 1998b.
33) Tanaka, H. and A. Thu : Full-range equation of friction coefficient and phase difference in a wave-current boundary layer, Coastal Eng., Vol.22, pp.237-254, 1994.

APPENDIX – NOTATIONS

The following symbols are used in this paper:

A = correlating coefficient;
A_{Ui} = component wave amplitude;
f = frequency of component waves;
f_w = wave friction factor;
$f_w(t)$ = instantaneous wave friction factor;
F_a = accuracy factor;
F_m = mean accuracy factor;
h = water depth;
$H_{1/3}$ = significant wave height;
H_U = velocity transfer function;
H_τ = transfer function between free stream velocity and bottom shear stress;
k = turbulent kinetic energy;
L = wave length;
n = correlating exponent;
N = total number of data points in accuracy factor computation;
p = pressure;
Re = wave Reynolds number;
$Re_{1/3}$ = wave Reynolds number corresponding to significant free stream velocity;

RE = Reynolds number corresponding to instantaneous free stream velocity;

S = reciprocal of Strouhal number;

S_U = spectral density of free stream velocity;

S_η = spectral density of irregular wave water surface elevation;

S_τ = spectral density of bottom shear stress;

t = time;

$T_{1/3}$ = significant wave period;

u = velocity in x- direction;

$-\overline{u'v'}$ = Reynolds stress;

U = free stream velocity;

$U(t)$ = instantaneous free stream velocity;

U_0 = maximum free stream velocity in an individual wave;

$U_{1/3}$ = significant free stream velocity;

x = co-ordinate along the flow;

z = co-ordinate perpendicular to the flow;

z_h = normalizing depth outside boundary layer;

Δf_i = frequency increment between successive wave components;

ϕ_i = component wave phases;

ε = dissipation rate of turbulent kinetic energy;

η = water surface elevation;

ν = kinematic viscosity of the fluid;

ν_t = turbulent viscosity;

θ = turbulent phase difference between free stream velocity and bottom shear stress;

ρ = mass density of the fluid;

σ = standard deviation of accuracy factor;

τ = shear stress;

τ_c = maximum bottom shear stress in an individual wave;

τ_0 = bottom shear stress;

$\tau_0(t)$ = instantaneous bottom shear stress;

ω = angular frequency of component waves; and

$\omega_{1/3}$ = angular frequency corresponding to significant wave period.

(Received July 19, 1999 ; revised September 14, 1999)